science, engineering and health studies

Research Article

Science, Engineering and Health Studies
https://lio1.tci-thaijo.org/index.php/sehs
ISSN (Online): 2630-0087

Development and evaluation of a fast dissolving effervescent microneedles patch for transdermal application

Phuvamin Suriyaamporn[1], Praneet Opanasopit[1], Tanasait Ngawhirunpat[1] and Worranan Rangsimawong[2]*

[1] Department of Pharmaceutical Technology, Faculty of Pharmacy, Silpakorn University, Nakhon Pathom 73000, Thailand
[2] Division of Pharmaceutical Chemistry and Technology, Faculty of Pharmaceutical Sciences, Ubon Ratchathani University, Ubon Ratchathani 34190, Thailand

***Corresponding author**: Worranan Rangsimawong worranan.r@ubu.ac.th*

***Received:** 4 April 2022*
***Revised:** 3 July 2022*
***Accepted:** 19 August 2022*
***Published:** 18 October 2022*

***Citation**: Suriyaamporn, P., Opanasopit, P., Ngawhirunpat, T., and Rangsimawong, W. (2022). Development and evaluation of a fast dissolving effervescent microneedles patch for transdermal application. Science, Engineering and Health Studies, 16, 22050010.*

ABSTRACT

The limitation of dissolving microneedles is the lengthy period of time to completely dissolve into the skin, so fast dissolving effervescent microneedles (Ef-MNs) have been developed. The objective of this study was to develop and evaluate the Ef-MNs as a device for transdermal application. The Ef-MNs were fabricated by a nonaqueous micromolding technique using poly (methyl vinyl ether/maleic acid) copolymers (GA), sodium bicarbonate, and various organic acids (citric acid, ascorbic acid, tartaric acid). The physical properties of the Ef-MNs were determined. The penetration depth was tested on neonatal porcine skin. The moisture determination of the Ef-MNs was investigated. For the results, all the formulations showed conical microneedles with 675.26 µm-height and 391.21 µm-width. In the mechanical strength, the Ef-MNs fabricated from ascorbic acid had a significantly higher resistance force than the others. As a result, all the Ef-MNs could be completely inserted into the skin. The dissolution study showed that the Ef-MNs fabricated from ascorbic acid were completely dissolved within 15 minutes and provided an appropriate moisture uptake and content. In conclusion, the optimal Ef-MNs were fabricated from 30% w/w of GA, 5% w/w of sodium bicarbonate, 5% w/w of ascorbic acid, and 60% w/w of ethanol, thus indicating an appropriate device for transdermal application.

Keywords: fast dissolving microneedles; effervescent microneedles; transdermal drug delivery; transdermal application

1. INTRODUCTION

The human skin is the largest organ of the body covering a surface area of approximately 1.7 m^2 (Menon, 2002). The delivery of drugs through the skin is an effective route of administration because of self-administration; it is safe, painless, and avoids the first pass metabolism in the gastrointestinal tract. However, transdermal drug delivery is limited by the stratum corneum, which is the physical barrier of the first layer of the skin, consequently leading to a decrease in the drug bioavailability and delivery effectiveness (Schoellhammer et al., 2014). The technologies used to modify the physical barrier of the stratum corneum can be divided into passive and active methods. Passive methods or chemical strategies, such as influence of drugs, vehicle interactions, optimization of formulation, and use of chemical enhancers could modify the structure of the stratum corneum barrier. However, main drawback of the

passive methods is poor efficacy (Alkilani et al., 2015). To overcome this problem, active methods such as fractional photothermolysis, sonophoresis, iontophoresis, thermophoresis, electroporation, and magnetophoresis have been recently used to enhance transdermal drug delivery by changing or bypassing the skin barrier (Gao et al., 2022). The limitations of these strategies are high cost of instruments and requirement of experienced people. Therefore, microneedles (MNs) have been developed to create microdimensions on the skin barrier for transportation of substance, thereby leading to improved bioavailability of drugs (Al-Zahrani et al., 2012).

MNs are micron scale technology (25-1000 μm in needle height) and can be inserted through the physical skin barrier (stratum corneum) into epidermis, thus improving transdermal drug delivery systems of various drugs, macromolecules, and nano/microparticles. As a consequence, this technology could improve bioavailability of transdermal drugs more than conventional preparations in the market, such as cream or gel, by about four-five times (Aung et al., 2020). MNs are also safe, painless, and easy to self-administer by the patients (Waghule et al., 2019). Normally, MNs are fabricated from many materials, such as metal, silicon, glass, polymer. The materials that are used to fabricate the microneedles for transdermal drug delivery should be inert, biocompatible, and have an appropriate mechanical strength and stability. In general, MNs can be divided into five types, depending on their range of size, shapes, materials produced, and their delivery mechanism (e.g., solid, coated, hollow, dissolving polymeric, and gel-forming MNs) (Mahato, 2017).

Dissolving polymeric MNs (DMNs), also called "poke and release", have received increased interest in the transdermal drug delivery field. This type of MNs is fabricated from biodegradable and biocompatible polymer. The drug is incorporated into the polymeric MNs and subsequent insertion into the skin. When the polymeric MNs contact with the fluid in the skin, the polymer matrix dissolves and releases the drug into the target site. The advantage of this type over solid, coated, and hollow MNs is the drug is completely dissolved with no biohazardous sharp waste, therefore providing dosing accuracy to reduce any side effects from high doses (Bhatnagar et al., 2019).

The number of the biodegradable and biocompatible polymers, including PVP, PVA, gelatin, hyaluronic acid, chitosan, and HPMC have been fabricated into the DMNs using simple molding techniques. However, poly(maleic diacid-alkyl vinyl ether) or poly (methyl vinyl ether/maleic acid) copolymers (GA) has high Young's modulus value when compared with other polymers, thus inferring highly stiff material. Moreover, the DMNs formulated using GA were reported to be strong and resist compression forces up to 0.7 N/needle without yielding (Eltayib et al., 2016). Furthermore, FDA-approved biocompatible polymers could be used to prepare the DMNs, which the GA had been widely used in the medical, cosmetic, and pharmaceutical fields with safety and low toxicity on the human skin (Burnett et al., 2011; Caló, 2016).

In addition, DMNs can be fabricated by using a simple and cost-effective method, which the appropriate physical properties to insert into the skin barrier and rapidly dissolve into the skin with a minimally invasive manner have been evaluated. The dissolution time of the DMNs depended on the type of polymer. For example, hyaluronic and carboxymethylcellulose (CMC) DMNs could completely dissolve >90% within 5-10 min after being applied on the skin (Leone et al., 2020; Ono et al., 2017). However, these polymers had low Young's modulus value or stiffness, so GA has beeb used for the fabrication of the DMNs. On the other hand, the dissolution times of GA after being applied on the skin was longer than 30 min, thus causing inconvenience for the users (Pamornpathomkul et al., 2018; Suriyaamporn et al., 2020). Therefore, fast dissolving effervescent MNs (Ef-MNs) patches have been developed to overcome this limitation.

The effervescent technique was the most effective and easy to formulate the DMNs than other techniques, such as two-layers separated backing MNs, controlled bubble sizes on the backing MNs, and polymeric porous MNs (Shi et al., 2021). At present, the novel technique of the effervescent principle or CO_2 bubble generation was used with the DMNs for increasing the dissolution time while being applied on the skin. Ke et al. (2012) studied the pH-responsive PLGA hollow microspheres with sodium bicarbonate ($NaHCO_3$) in an aqueous core shell loaded in polyvinylpyrrolidone (PVP) DMNs. When the hollow microspheres loaded in the PVP DMNs were applied on the skin (acidic environment; pH 5.5), they rapidly reacted with $NaHCO_3$ and formed a large number of CO_2 bubbles, which affected the dissolution time. Moreover, Ning et al. (2021) fabricated the bubble-generating DMNs by mixing citric acid and $NaHCO_3$ in the PVP DMNs. After that, the formulations of the DMNs were coated with poly(ethylene glycol) (PEG) and poly(lactic-co-glycolic acid) (PLGA) to control the rate of the bubble generation. Upon insertion into the skin, interstitial fluid of the skin could diffuse into the DMNs. Therefore, the citric acid was exposed to $NaHCO_3$ and produced CO_2 bubbles for the increased dissolution time. Finally, the effervescent technique was used in the fabrication of the long-acting DMNs. The effervescence mixture junction between the tips and patch of the DMNs was fabricated from citric acid, $NaHCO_3$ and PVP. The tips of the needle were rapidly separated from the patch within the skin when contacted with interstitial fluid of the skin caused by the generation of CO_2 bubbles (Li et al., 2019).

The Ef-MNs patches were designed to dissolve in water. These MNs were fabricated from organic acids and carbonate/bicarbonate salt using a nonaqueous micromolding technique to prevent a pre-effervescent reaction. Citric acid, ascorbic acid, and tartaric acid were the natural organic acid compounds that were safe and popular to produce the effervescent products. Additionally, these organic acids did not absorb humidity at 25°C/65% RH (Rowe et al., 2009). The reaction of the organic acids and salts in the interstitial fluid of the skin could release CO_2 bubbles, consequently leading to increased dissolution times faster than the conventional DMNs without involving a failure of the mechanical strength (Li et al., 2019). However, the effect of the different natural organic acid compounds on the Ef-MNs properties have not yet been clarified.

The objective of this study was to develop and evaluate the Ef-MNs patches as a device for transdermal application. The Ef-MNs were fabricated by nonaqueous micromolding using GA polymer, N_aHCO_3, and various organic acids (citric acid, ascorbic acid, tartaric acid). The physical appearance and mechanical strength of the Ef-MNs were determined. The dissolution time, percent insertion, and penetration depth were tested on neonatal porcine skin. Finally, the moisture determination of the Ef-MNs was also investigated.

2. MATERIALS AND METHODS

2.1 Materials

Poly (methyl vinyl ether/maleic acid) copolymers (GA; Gantrez™ S-97 BF; MW 1,500 kDa) were purchased from Ashland Inc. (Surrey, UK). $NaHCO_3$ and citric acid were obtained from Ajax Finechem Pty. Ltd. (Seven Hills, Australia). Ascorbic acid was purchased from Riedel-de Haën® (Seelze, Germany). Tartaric acid was purchased from Grand Chemicals Far East Co., Ltd. (Bangkok, Thailand). Phosphate buffered saline (PBS; 1X; pH 7.4) was prepared from 8 g/L of NaCl, 0.2 g/L of KCl, 1.44 g/L of Na_2HPO_4 (anhydrous), and 0.25 g/L of KH_2PO_4 (anhydrous). Fresh neonatal porcine skin was received from a slaughterhouse in Nakhon Pathom Province, Thailand. All the chemical agents and solvents were an analytical reagent grade.

2.2 Fabrication of the Ef-MNs patches

GA was dissolved in pure ethanol to obtain 30% w/w of polymer solution. After that, various organic acids and sodium bicarbonate were mixed in the GA solution (Table 1). Approximately 500 mg of the mixed polymer solutions were poured into the polydimethylsiloxane micro-mold (Blueacre Technology, Ireland). Each micromold consisted of 121 conical needles (11×11 arrays) with a height of 600 µm, base diameter of 300 µm, and interspacing of 300 µm. Then, the MNs formulations were centrifuged (ALC, PK121R, UK) at 4,000 rpm, at a temperature of 25°C for 20 min to remove the air bubbles. The mold was placed in a vacuum chamber (TÜV Rheinland, Thailand) for 30 min (60 psi; 25°C) to fill the sample in the microneedle cavities. All the formulations were completely dried in a desiccator to prevent pre-effervescence at a temperature of 25°C for 48 h. Then the Ef-MNs patches were gently removed from the micromold, and then stored in the desiccator to prevent air humidity. Finally, the Ef-MN patches were exposed to low-intensity ultraviolet light for 5 min (360 nm; ~2mW per cm^2) to sterilize and eliminate any microorganisms (Than et al., 2018).

Table 1. The formulations of fast dissolving effervescent microneedles

Formulation	GA (%w/w)	$NaHCO_3$ (%w/w)	Citric acid (%w/w)	Ascorbic acid (%w/w)	Tartaric acid (%w/w)	Ethanol qs to
GA-MNs	30	-	-	-	-	100
Ef-MNs1	30	5	5	-	-	100
Ef-MNs2	30	5	-	5	-	100
Ef-MNs3	30	5	-	-	5	100

2.3 Morphology of the Ef-MNs patches

The morphology of each formulation of the Ef-MNs patch and GA-MNs patch was evaluated using a Dino-Lite Edge/5MP digital microscope, AM7915 series (Dino-Lite, Hsinchu, Taiwan). The height and base width of the needles were initially measured using Dinocapture 2.0 software.

2.4 Mechanical properties of the Ef-MNs patches

The mechanical strength of the Ef-MNs patches played an important factor in the practical use of the MNs. The strength or hardness of the Ef-MNs patches was measured by a texture analyzer (TA.XT plus, Stable Micro Systems, UK) connected to a 5-kg load cell. The compression mode was used to evaluate the Ef-MNs patches. The Ef-MNs patches kept at room temperature, in a desiccator with calcium chloride ($CaCl_2$), were mounted on a stainless-steel cylinder probe (P/10KSS) in a vertical position. The probe was moved down and up at the same rate of 1 mm/s and pressed on the Ef-MNs patch with constant increased force until the displaced height of the Ef-MNs patches was around 0.8 mm. The force versus the height displacement curves were plotted to evaluate the highest mechanical strength of the Ef-MNs patches.

2.5 Preparation of the neonatal porcine skin

The full thickness neonatal porcine skins, received from a slaughterhouse in Nakhon Pathom Province (Thailand), were used in this study because they were the best representative of human skin (the thickness ~900±190 µm) (Simon and Maibach, 2000). The neonatal porcine stratum corneum at the first layer of the skin was more similar to that of human skin when compared with adult porcine skin. The neonatal porcine skins were excised, the subcutaneous fat was removed, and then were stored at a temperature of -20°C for further use. Prior to the experiment, the neonatal porcine skins were cleaned and warmed with PBS (pH 7.4) at a temperature of 37°C. After that, the neonatal porcine skins were dried and used in the experiment.

2.6 Insertion and penetration depth of the Ef-MNs patches

The insertion ability was an important factor for developing the Ef-MNs patches, which the Ef-MNs should overcome the skin barrier, which led to efficiently delivering the substance into the skin. The evaluation of the Ef-MNs patches skin insertion and penetration depth was performed using fresh neonatal porcine skin as an alternative human skin model. The Ef-MNs patches were applied on the neonatal porcine skin with a strength of a 2-kg dumbbell for 30 s and removed. The 2 kg (20 N) of strength represented the average human's press force (Larrañeta et al., 2014). The 1% methylene blue was dropped on the damaged neonatal porcine skin for 5 min. Then, the damaged points of the neonatal porcine skin were evaluated under Dino-Lite digital microscope and calculated the % complete insertion as shown in Equation 1.

$$\% \text{ Complete insertion} = \frac{\text{Number of dots on the porcine skin}}{\text{Number of microneedles arrays}} \times 100 \qquad (1)$$

To study the penetration depth, 1% of fluorescein sodium was loaded onto the Ef-MNs patches and applied on the neonatal porcine skin with a strength of 2 kg for 30 s. The neonatal porcine skin was fixed with Carnoy's solution for 30 min and then embedded with a tissue freezing medium at a temperature of -80°C for 2 h. The treated neonatal porcine skin was cross-sectioned into 20 µm using a cryostat (CM1850, Leica Biosystems, Germany), and the sliced skin tissues were placed onto glass slides. The cross-sectioned skin was immediately evaluated under a fluorescence microscope (Nikon® T-DH; Japan) with an emission intensity at 520 nm. The cross-sectioned skin was also evaluated under a bright field mode. The images were captured with a 10× objective lens.

2.7 Dissolution time of the Ef-MNs patches

The appropriate dissolution time points on the neonatal porcine skin to investigate if the microneedle could completely dissolve and diffuse into the skin were evaluated. The dissolution rates of the Ef-MNs' arrays were dependent on the types of the organic acids. To confirm the time of dissolution, the neonatal porcine skin was shaved, and the skin's subcutaneous fat was removed. The neonatal porcine skin was stretched on saturated PBS pH 7.4 tissue paper. The Ef-MNs patches were applied on the neonatal porcine skin with a strength of 2 kg for 30 s and placed in the incubator cabinet at a temperature of 37°C. The Ef-MNs patches were collected and removed from the neonatal porcine skin at time periods of 0, 5, 15, 20, and 30 min, respectively. The height appearance of the Ef-MNs patches was observed under the digital microscope. After that, the remaining height of the Ef-MNs was calculated and reported as %height remaining versus time as shown in Equation 2. The threshold for considering the complete dissolution of the Ef-MNs patches was more than 10% of the remaining height after being applied on the skin at the determined time (Albadr et al., 2022; Aung et al., 2020; Suriyaamporn et al., 2021).

$$\%\ \text{Height remaining} = \frac{\text{Height before being applied on the skin} - \text{Height after being applied on the skin}}{\text{Height before being applied on the skin}} \times 100 \qquad (2)$$

Moisture determination of the Ef-MNs patches: The moisture uptake and content were one of the most important parameters for measuring the polymeric MNs formulations. The air humidity might affect the efficiency of the Ef-MNs patch. The Ef-MNs patches were accurately weighed and kept in a desiccator containing the saturated solution of potassium chloride (KCl) to maintain 85% RH for the calculation of the percentage of the moisture uptake and that containing fused calcium chloride ($CaCl_2$) to maintain 22% RH for the calculation of the percentage of the moisture content at a temperature of 25°C for 24 h (Mahajan et al., 2018). After 24 h, the Ef-MNs patches were reweighed and calculated as shown in Equations 3 and 4.

$$\%\ \text{Moisture uptake} = \frac{\text{Final weight } (W_2) - \text{Initial weight } (W_1)}{\text{Initial weight } (W_1)} \times 100 \qquad (3)$$

$$\%\ \text{Moisture content} = \frac{\text{Final weight } (W_2) - \text{Initial weight } (W_1)}{\text{Final weight } (W_2)} \times 100 \qquad (4)$$

2.8 Statistical analysis

Each study was performed in triplicate, and the results were presented as the mean±standard deviation (SD). The Anderson-Darling test was used to test the normality of the data. For the comparison of the two groups, an independent two-sided t-test was used. Statistical analysis of the calculated multiple groups was performed by a one-way ANOVA test with a post hoc Tukey's test. SPSS® software version 19 (SPSS Inc., Chicago, IL) was used in this study. The results were considered to be significant at p-values < 0.05.

3. RESULTS AND DISCUSSION

3.1 Morphology of the Ef-MNs patches

All the formulations could be completely fabricated to be 121 needles with a patch size of 5×5 mm^2 (11 rows x 11 columns), which the average height was around 675.26±20.67 µm, base needle width around 391.21±23.57 µm, and interneedle spacing of around 600.10±0.21 µm (Table 2). Because of the thickness of the skin tissue of around 900±190 µm, the morphology of the Ef-MNs patches was appropriate for penetrating into the skin at an acceptable height range. Moreover, the Ef-MNs height did not reach the nerves and blood supply, thus providing minimal invasion and was painless (Waghule et al., 2019). The Ef-MNs1 that was fabricated from the citric acid showed many air bubbles on the backing layer, as the hygroscopic effect of the citric acid affected the pre-effervescence during the drying process.

3.2 Mechanical properties of the Ef-MNs patches

For the mechanical strength, only 30% GA microneedles (GA-MNs) had the highest resistance force of around 53.3 N, when compared with all the formulations of the Ef-MNs patches. However, the Ef-MNs2 fabricated from ascorbic acid had a significantly higher resistance force (45 N) than other formulations of the Ef-MNs patches (Figure 1). Nonetheless, the minimum insertion force of the microneedles used to penetrate into the human skin was about 0.1-3.0 N (Prausnitz, 2004). This suggested that the hygroscopic effect of the Ef-MNs patches influenced the microneedles strength because the organic acids and salts of the EF-MNs patches easily absorbed moisture after being exposed to humidity (Violalita and Rini, 2015). The hygroscopic effect of the organic acids could be explained by polar or charged functional groups that were bonded with molecules of water. In addition, citric acid had four functional groups (three carboxyl groups and one hydroxyl group), thereby indicating a higher hygroscopicity than tartaric acid (two carboxyl groups and two hydroxyl groups) and ascorbic acid (four hydroxyl groups),

respectively (Rowe et al., 2009). Nevertheless, the mechanical strength of all the formulations of the Ef-MNs patches after moisture control (MC) by storing in the desiccator with $CaCl_2$ at a temperature of 25°C was increased; however, there was no significant difference from those without MC. Nevertheless, this device was kept in the desiccator or avoided air humidity to prevent pre-effervescence.

Table 2. Physical appearance and insertion study of microneedle formulations

	MNs formulations			
	GA-MNs	**Ef-MNs1**	**Ef-MNs2**	**Ef-MNs3**
Physical appearance	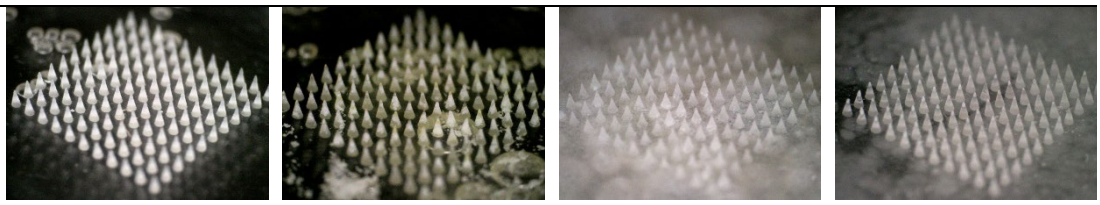			
Insertion	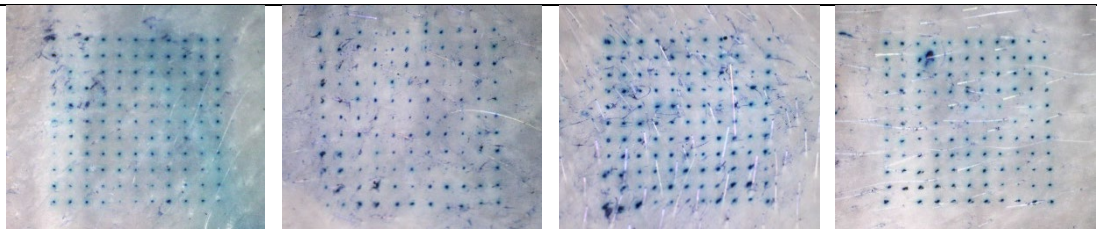			

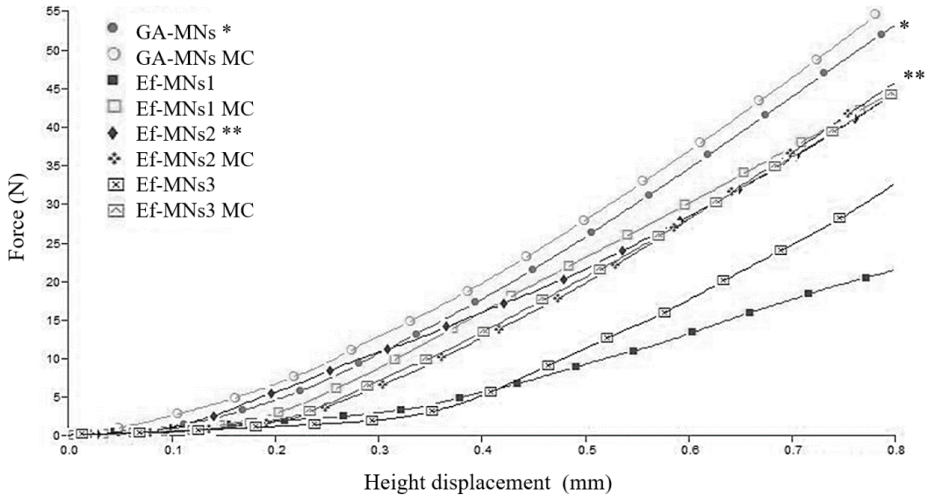

Figure 1. The force versus height displacement of microneedle formulations
Note: * indicated significantly higher than other formulations ($p < 0.05$). ** indicated significantly higher than other Ef MNs patch formulations ($p < 0.05$).

3.3 Insertion and penetration depth of the Ef-MNs patches

To overcome the stratum corneum barrier, the insertion and penetration depth were tested on neonatal porcine skin, which the structure properties of the neonatal porcine skin were similar to human skin (Simon and Maibach, 2000). As shown in Table 2, all the MNs formulations could completely create the damaged point on the neonatal porcine skins. This indicated that all the formulations of the EF-MNs patch showed successful insertion (100%) into the skin without any mechanical failure when compared with the control (GA-MNs patch). The cross-section image of the skin after the insertion of the Ef-MNs2 that had appropriate characterization showed the observed length of around 505.66 ± 5.04 μm, thus suggesting that the formulations of the Ef-MNs patch could create micro-channels bypassing the stratum corneum barrier and leading to enhancing the transdermal delivery of the drugs (Figure 2). This formulation of the Ef-MNs patch could reach the target site or dermis of the skin; therefore, the drug substance could be delivered by these MNs formulations. Moreover, the blood and nerves supply had a depth of more than 2 mm from the skin surface, consequently resulting in no pain or infection being found in this Ef-MN height (Alkilani et al., 2015).

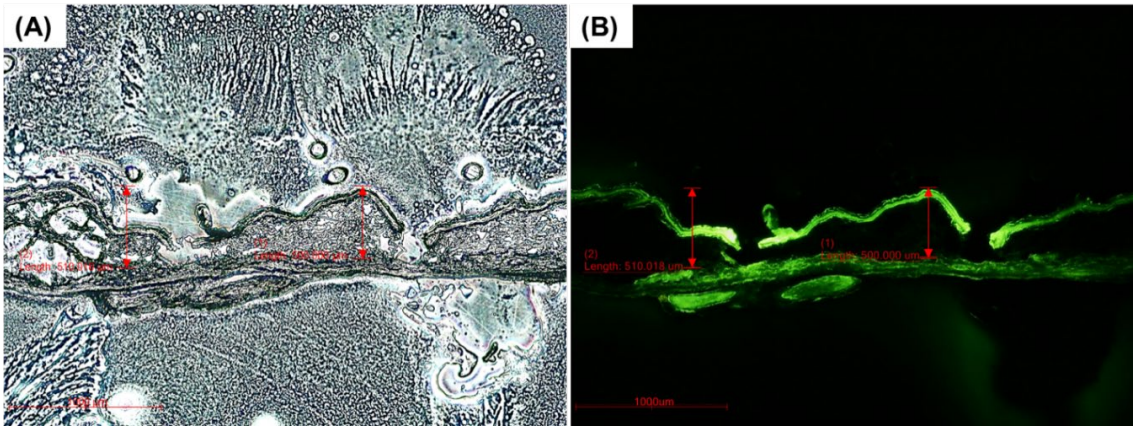

Figure 2. Depth of insertion of the skin cross section obtained after Ef-MNs2 patch insertion; (A) bright field image and (B) fluorescent image

3.4 Dissolution time of the Ef-MNs patches

The dissolution time was one of the important factors for developing the Ef-MNs patches. Theoretically, the Ef-MNs patches were dissolved after close contact with the interstitial fluid under the skin barrier (Yao et al., 2017). As shown in Table 3 and Figure 3, all the Ef-MNs patches completely dissolved faster than the control (GA-MNs). Upon applying the Ef-MNs patches on the neonatal porcine skin, the Ef-MNs patches absorbed water from the saturated PBS tissue paper and generated CO_2 bubbles from the reaction between the organic acid and sodium bicarbonate (Equations 5-7).

Citric acid: $C_6H_8O_{7(aq)} + 3NaHCO_{3(aq)} \rightarrow 3CO_{2(g)} + 3H_2O_{(l)} + Na_3C_6H_5O_{7(aq)}$ (5)

Ascorbic acid: $C_6H_8O_{6(aq)} + NaHCO_{3(aq)} \rightarrow CO_{2(g)} + H_2O_{(l)} + NaC_6H_7O_{6(aq)}$ (6)

Tartaric acid: $C_4H_6O_{6(aq)} + 2NaHCO_{3(aq)} \rightarrow 2CO_{2(g)} + 2H_2O_{(l)} + Na_2C_4H_4O_{6(aq)}$ (7)

Table 3. Dissolution time points of microneedle formulations

	Dissolution time points (min)				
	0	**5**	15	**20**	**30**
GA-MNs	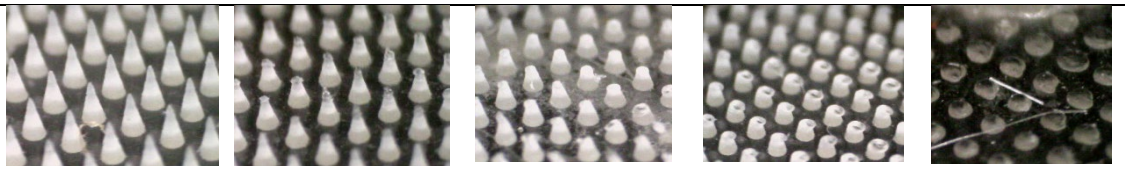				
Ef-MNs1	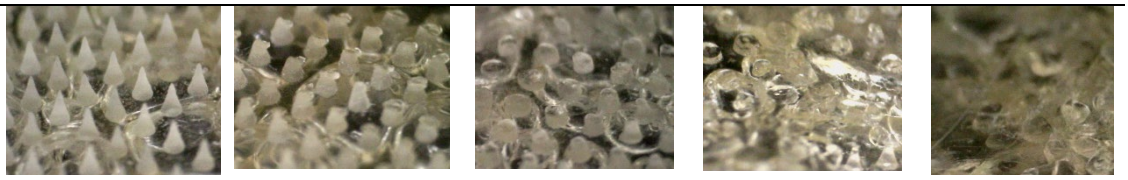				
Ef-MNs2	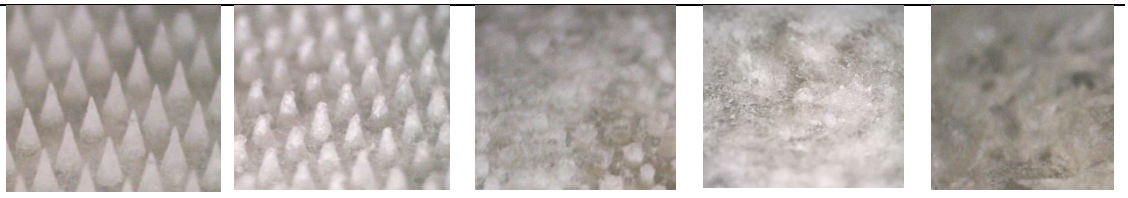				
Ef-MNs3	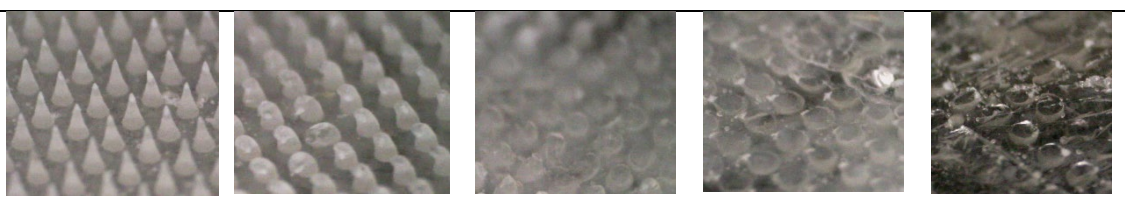				

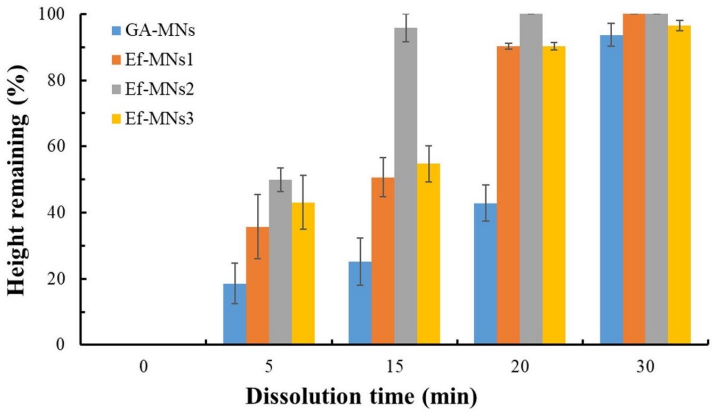

Figure 3. Percentage of the height remaining of Ef-MNs patches in the porcine skin versus predefined dissolution time (n = 3)
Note: * indicated significantly higher than other formulations ($p < 0.05$).

Hence, the Ef-MNs patches were mechanically weakened and broken by the CO_2 bubbles, thus leading to fast dissolving microneedles. From this result, the dissolution time at 15 min to completely dissolve the Ef-MNs2 patch was significantly higher than the control, Ef-MNs1 patch, and Ef-MNs3 patch, indicating that ascorbic acid in the Ef-MN2 patch provided a faster dissolution time than the citric acid and tartaric EF-MNs patches. Moreover, the Ef-MNs1 patch and Ef-MNs3 patch could be completely dissolved within 20 min, while the GA-MNs was done within 30 min. This suggested that ascorbic acid had low or no hygroscopicity, thereby leading to less or no pre-effervescent effect during the drying process which effected the dissolution time when compared to the other formulations. This ascorbic acid in the Ef-MN2 patch could be helpful in the formulation because it was easier to handle (Parikh, 2021).

The effect of the different natural organic acid compounds on the Ef-MNs properties have not yet been clarified. The other studies mostly used citric acid as organic acid compounds for the effervescent effect (Ke et al., 2012; Li et al., 2019; Ning et al., 2021). Therefore, ascorbic acid was recommended as the organic acid compounds for increasing the dissolution time with low or no hygroscopicity when applied on the skin.

3.5 Percentage of the moisture uptake and moisture content of the Ef-MNs patches

The moisture uptakes and content were important factors affecting the mechanical properties of the Ef-MNs patches, including rigidity, flexibility, and dissolution kinetic within the skin tissues that could affect the drug stability and efficacy. The high content of the moisture in the air humidity impaired the Ef-MNs patches ability to penetrate the skin tissue. The percentage of the moisture uptake of all the formulations was in the following order: Ef-MNs1 patch (16.15±0.45%) > Ef-MNs3 patch (15.20±2.73%) > Ef-MNs2 patch (10.65±3.70%) > GA-MNs patch (9.68±0.40%), while the percentage of the moisture content was in the following order: Ef-MNs1 patch (4.66±0.26%) > Ef-MNs3 patch (3.71±0.48%) > Ef-MNs2 patch (1.91±0.25%) > GA-MNs patch (1.74±0.65%). The Ef-MNs1 patch showed the highest moisture uptake and content. This result suggested that the hygroscopic effect of organic acid affected the percentage of the moisture uptake and content of the Ef-MNs patches (Rowe et al., 2009). The citric acid and tartaric acid Ef-MNs patch formulations had moisture uptake of more than 15% at 25°C/80% RH, hence representing very high hygroscopicity (Newman et al., 2008). Therefore, the moisture uptake and content of the Ef-MNs2 patch were lower than other Ef-MNs patch formulations and were not significantly different from the control. Therefore, the Ef-MNs2 patch was an appropriate fast dissolving formulation as a microneedle device for transdermal application.

The Ef-MNs could result an effervescence reaction before being used by inappropriate storage, which affected the mechanical strength and dissolution time. Hence, the Ef-MNs should be kept in strong airtight packaging to prevent pre-effervescence and protect the needle tip that might be damaged before being used (McAlister et al., 2021).

4. CONCLUSION

The fast-dissolving Ef-MNs as a transdermal drug delivery approach was a new concept of MNs fabrication. The optimal Ef-MNs patch formulation was fabricated from 30% w/w of GA, 5% w/w of $NaHCO_3$, and 5% w/w of ascorbic acid as an appropriate device for transdermal application. These Ef-MNs patches were fabricated by a simple and cost-effective nonaqueous micromold casting method that used an economic biocompatible polymer. This exhibited a suitable physical appearance and mechanical strength, as well as successful insertion into the skin with a depth of 505.66 µm. This suggested that this Ef-MNs patch could create micro-channels bypassing the stratum corneum barrier, thus leading to enhance the transdermal delivery of the drugs. Moreover, this Ef-MNs patch was completely dissolved in the skin within 15 min, and had the lowest moisture uptake and content, when compared with other Ef-MNs patch formulations. Therefore, the optimal Ef-MNs fabricated from GA, sodium bicarbonate. and ascorbic acid were as suitable as a fast-dissolving MNs device for transdermal application. In the future, studies should be carried out to determine whether these MNs have the potential to be a transdermal delivery device for other active pharmaceutical ingredients, such as hydrophilic compounds that could be compatible with water soluble polymer.

ACKNOWLEDGMENT

The authors would like to thank the National Research Council of Thailand (NRCT; Grant No. N42A650551) for financial support.

REFERENCES

Albadr, A. A., Tekko, I. A., Vora, L. K., Ali, A. A., Laverty, G., Donnelly, R. F., and Thakur, R. R. S. (2022). Rapidly dissolving microneedle patch of amphotericin B for intracorneal fungal infections. *Drug Delivery and Translational Research*, 12(4), 931-943.

Alkilani, A. Z., McCrudden, M. T. C., and Donnelly, R. F. (2015). Transdermal drug delivery: Innovative pharmaceutical developments based on disruption of the barrier properties of the stratum corneum. *Pharmaceutics*, 7(4), 438-470.

Al-Zahrani, S., Zaric, M., McCrudden, C., Scott, C., Kissenpfennig, A., and Donnelly, R. F. (2012). Microneedle-mediated vaccine delivery: harnessing cutaneous immunobiology to improve efficacy. *Expert Opinion on Drug Delivery*, 9(5), 541-550.

Aung, N. N., Ngawhirunpat, T., Rojanarata, T., Patrojanasophon, P., Pamornpathomkul, B., and Opanasopit, P. (2020). Fabrication, characterization and comparison of alpha-arbutin loaded dissolving and hydrogel forming microneedles. *International Journal of Pharmaceutics*, 586, 119508.

Bhatnagar, S., Gadeela, P. R., Thathireddy, P., and Venuganti, V. V. K. (2019). Microneedle-based drug delivery: materials of construction. *Journal of Chemical Sciences*, 131, 90.

Burnett, C. L., Bergfeld, W. F., Belsito, D. V., Hill, R. A., Klaassen, C. D., Liebler, D. C., and Andersen, F. A. (2011). Final report of the Amended Safety Assessment of PVM/MA copolymer and its related salts and esters as used in cosmetics. *International Journal of Toxicology*, 30(Suppl), 128s-144s.

Eltayib, E., Brady, A. J., Caffarel-Salvador, E., Gonzalez-Vazquez, P., Zaid Alkilani, A., McCarthy, H. O., and Donnelly, R. F. (2016). Hydrogel-forming microneedle arrays: Potential for use in minimally-invasive lithium monitoring. *European Journal of Pharmaceutics and Biopharmaceutics*, 102, 123-131.

Caló, E., Barros, J., Ballamy, L., and Khutoryanskiy, V. V. (2016). Poly(vinyl alcohol)–Gantrez® AN cryogels for wound care applications. *RSC Advances*, 6(107), 105487.

Gao, Y., Du, L., Li, Q., Zhu, L., Yang, M., and Ma, S. (2022). How physical techniques improve the transdermal permeation of therapeutics: A review. *Medicine*, 101(26), e29314.

Ke, C. J., Lin, Y. J., Hu, Y. C., Chiang, W. L., Chen, K. J., Yang, W. C., and Sung, H. W. (2012). Multidrug release based on microneedle arrays filled with pH-responsive PLGA hollow microspheres. *Biomaterials*, 33(20), 5156-5165.

Larrañeta, E., Moore, J., Vicente-Pérez, E. M., González-Vázquez, P., Lutton, R., Woolfson, A. D., and Donnelly, R. F. (2014). A proposed model membrane and test method for microneedle insertion studies. *International Journal of Pharmaceutics*, 472(1-2), 65-73.

Leone, M., Romeijn, S., Slütter, B., O'Mahony, C., Kersten, G., and Bouwstra, J. A. (2020). Hyaluronan molecular weight: Effects on dissolution time of dissolving microneedles in the skin and on immunogenicity of antigen. *European Journal of Pharmaceutical Sciences*, 146, 105269.

Li, W., Tang, J., Terry, R. N., Li, S., Brunie, A., Callahan, R. L., and Prausnitz, M. R. (2019). Long-acting reversible contraception by effervescent microneedle patch. *Science Advances*, 5(11), eaaw8145.

Mahajan, N. M., Zode, G. H., Mahapatra, D. K., Thakre, S., Dumore, N., and Gangane, P. S. (2018). Formulation development and evaluation of transdermal patch of piroxicam for treating dysmenorrhoea. *Journal of Applied Pharmaceutical Science*, 8(11), 35-41.

Mahato, R. (2017). Microneedles in drug delivery. In *Emerging Nanotechnologies for Diagnostics, Drug Delivery and Medical Devices* (Mitra, A. K., Cholkar, K., and Mandal, A., eds.), 1st, pp. 331-349. Amsterdam: Elsevier.

McAlister, E., Kearney, M. C., Martin, E. L., and Donnelly, R. F. (2021). From the laboratory to the end-user: a primary packaging study for microneedle patches containing amoxicillin sodium. *Drug Delivery and Translational Research*, 11(5), 2169-2185.

Menon, G. K. (2002). New insights into skin structure: scratching the surface. *Advanced Drug Delivery Reviews*, 54 (Suppl), S3-S17.

Newman, A. W., Reutzel-Edens, S. M., and Zografi, G. (2008). Characterization of the "hygroscopic" properties of active pharmaceutical ingredients. *Journal of Pharmaceutical Sciences*, 97(3), 1047-1059.

Ning, X., Chen, S., Yang, Y., Hwang, J., Wiraja, C., Zhang, C., and Xu, C. (2021). Photodynamic bubble-generating microneedles for enhanced transdermal cancer therapy. *ACS Applied Polymer Materials*, 3(12), 6502-6512.

Ono, A., Ito, S., Sakagami, S., Asada, H., Saito, M., Quan, Y. S., and Okada, N. (2017). Development of novel faster-dissolving microneedle patches for transcutaneous vaccine delivery. *Pharmaceutics*, 9(3), 27.

Pamornpathomkul, B., Ngawhirunpat, T., Tekko, I. A., Vora, L., McCarthy, H. O., and Donnelly, R. F. (2018). Dissolving polymeric microneedle arrays for enhanced site-specific acyclovir delivery. *European Journal of Pharmaceutical Sciences*, 121, 200-209.

Parikh, D. M. (2021). *Handbook of Pharmaceutical Granulation Technology* (4th ed.). Florida: CRC Press.

Prausnitz, M. R. (2004). Microneedles for transdermal drug delivery. *Advanced Drug Delivery Reviews*, 56(5), 581-587.

Rowe, R. C., Sheskey, P. J., and Quinn, M. E. (2009). *Handbook of Pharmaceutical Excipients* (6th ed.), Vol. 1. London: Pharmaceutical Press.

Schoellhammer, C. M., Blankschtein, D., and Langer, R. (2014). Skin permeabilization for transdermal drug delivery: recent advances and future prospects. *Expert Opinion on Drug Delivery*, 11(3), 393-407.

Shi, Y., Lu, A., Wang, X., Belhadj, Z., Wang, J., and Zhang, Q. (2021). A review of existing strategies for designing long-acting parenteral formulations: Focus on underlying mechanisms, and future perspectives. *Acta Pharmaceutica Sinica B*, 11(8), 2396-2415.

Simon, G. A., and Maibach, H. I. (2000). The pig as an experimental animal model of percutaneous permeation in man: qualitative and quantitative observations-an overview. *Skin Pharmacology and Physiology*, 13(5), 229-234.

Suriyaamporn, P., Opanasopit, P., Ngawhirunpat, T., and Rangsimawong, W. (2021). Computer-aided rational design for optimally Gantrez® S-97 and hyaluronic

acid-based dissolving microneedles as a potential ocular delivery system. *Journal of Drug Delivery Science and Technology*, 61, 102319.

Suriyaamporn, P., Rangsimawong, W., Opanasopit, P., and Ngawhirunpat, T. (2020). Development and characterization of Gantrez® S-97 and hyaluronic acid microneedles for transdermal fluorescein sodium delivery. *Key Engineering Materials*, 859, 125-131.

Than, A., Liu, C., Chang, H., Duong, P. K., Cheung, C. M. G., Xu, C., and Chen, P. (2018). Self-implantable double-layered micro-drug-reservoirs for efficient and controlled ocular drug delivery. *Nature Communications*, 9(1), 4433.

Violalita, F., and Rini, B. (2015). The effect acid addition on characteristic effervescent tablet of tamarillo. *International Journal on Advanced Science, Engineering and Information Technology*, 5(3), 230-233.

Waghule, T., Singhvi, G., Dubey, S. K., Pandey, M. M., Gupta, G., Singh, M., and Dua, K. (2019). Microneedles: A smart approach and increasing potential for transdermal drug delivery system. *Biomedicine & Pharmacotherapy*, 109(3), 1249-1258.

Yao, G., Quan, G., Lin, S., Peng, T., Wang, Q., Ran, H., and Wu, C. (2017). Novel dissolving microneedles for enhanced transdermal delivery of levonorgestrel: *In vitro* and *in vivo* characterization. *International Journal of Pharmaceutics*, 534(1-2), 378-386.